

V.S. Trush¹, N.N. Pylypenko², P.I. Stoev², M.A. Tikhonovsky², I.M. Pohrelyuk¹,
V.M. Fedirko¹, A.G. Luk'yanenko¹, S.M. Lavrys¹

Influence of interstitial elements (oxygen, nitrogen) on properties of zirconium alloys (review)

¹Karpenko Physico-Mechanical Institute of the NAS of Ukraine, Lviv, Ukraine

²National Science Center "Kharkov Institute of Physics and Technology" of the NAS of Ukraine, Kharkiv, Ukrain,
trushvasyl@gmail.com

A review of the regularities of the influence of interstitial elements (oxygen, nitrogen) on the properties of zirconium alloys was presented. It was noted that in the scientific and technical literature dates the main attention is paid to the bulk alloying of zirconium alloys with oxygen and nitrogen at high temperatures. It was shown that zirconium with nitrogen and oxygen forms a number of stable compounds of suboxides and subnitrides. The physico-mechanical characteristics of zirconium after heat treatment under media containing both oxygen and nitrogen components on the properties of zirconium alloys were analysed.

Keywords: zirconium alloys, oxygen, nitrogen, solubility, physical and mechanical properties.

Received 15 March 2022; Accepted 23 June 2022.

Introduction

Zirconium alloys are important structural materials for components of fuel cladding and structural components for light and heavy water nuclear reactor cores because of their low capture cross-section to thermal neutrons and their good corrosion resistance. [1–3]. In the detection of safety, increased requirements are needed to the fuel-rod elements of nuclear reactors. The most vulnerable element of fuel-pod is the cladding (wall) of tubes made of zirconium alloys (fig. 1).

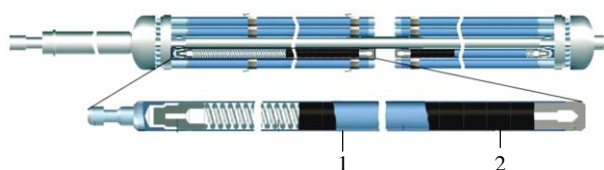


Fig.1. Schematic of nuclear fuel rod [4-5]:
1 – zirconium cladding; 2 – uranium dioxide tablet

The use of zirconium-based alloys as domestic structural materials for nuclear reactors requires

knowledge of the patterns of formation of the phase-structural state of the near-surface layer of metal during thermochemical treatment, which is used as the finishing treatment in manufacturing of fuel-pod element [1,2]. The interstitial elements (oxygen, nitrogen and hydrogen) have a significant influence on the performance of zirconium.

I. I.Basis of interaction of interstitial elements (o, n, h) with zirconium

The solubility of the interstitial elements (oxygen, nitrogen, hydrogen) in zirconium is of particular practical importance. According to phase diagrams (fig. 2), the oxygen has the highest solubility in α -zirconium – 28% at., then nitrogen – 22% at. and hydrogen – the smallest (7% at.). The high solubility of oxygen in zirconium makes this interstitial element promising for practical use – alloying with oxygen as control method of structure in the Zr–O system and the properties of zirconium and its alloys. Only oxygen is considered not only as a harmful impurity but also as an alloying element.

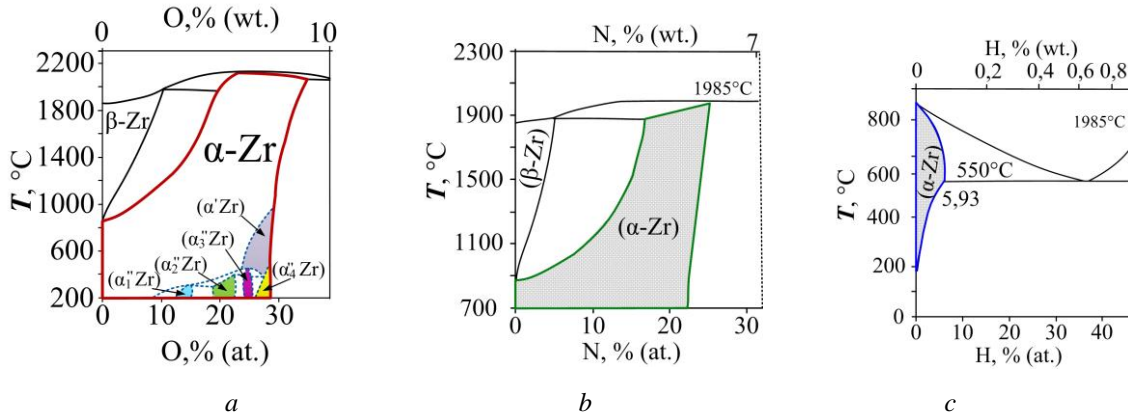


Fig. 2. Part of phase diagram: a – «Zr – O» [6]; b – «Zr – N» [7]; c – «Zr – H» [8].

In terms of diffusion mobility in zirconium, hydrogen exceeds oxygen and nitrogen. Distinctive features of the diffusion of hydrogen from the diffusion of other interstitial elements (for example, O, N, C) are, firstly, the extremely low activation energy and, secondly, the quantum diffusion nature in a wide temperature ranges up to room temperature (fig. 3) [9,10].

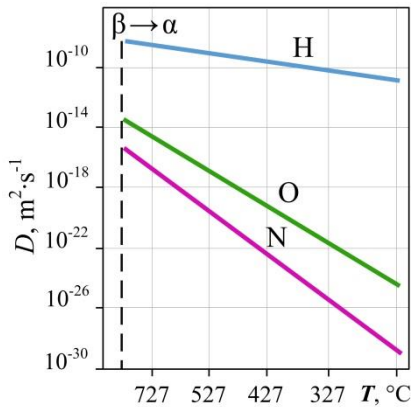


Fig. 3. Diffusion coefficients of oxygen, nitrogen and hydrogen in α -Zr [9, 10].

It should be noted that the interstitial elements, penetrating into the zirconium matrix, lead to a change in the crystal lattice parameters [11] and increase the region of existence of the Zr α -phase (fig. 4). For example, the oxygen content up to 30% at. causes a change in the c/a ratio from 1.598 to 1.602, and the presence of oxygen in an amount of up to 2.5% wt. increases the polymorphic transformation temperature of zirconium by 400°C [12].

The limiting solubility of oxygen, nitrogen and carbon is shown in fig. 5 [13]. Zirconium forms strong compounds with nitrogen and oxygen. Therefore, it is impossible to reduce the content of the above mentioned impurities in zirconium by the main mechanisms of removal of diatomic gases during electron beam melting in a vacuum. This mainly concerns the removal of nitrogen from zirconium. It is possible to reduce the nitrogen content in zirconium only at the previous stage of reduction.

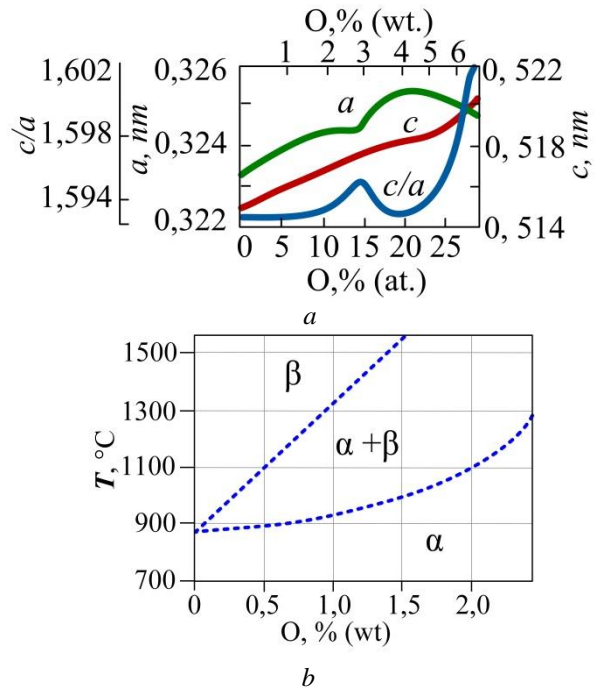


Fig. 4. Effect of oxygen on characteristics of zirconium: (a) lattice parameters [11], (b) polymorphic transformation temperature [12].

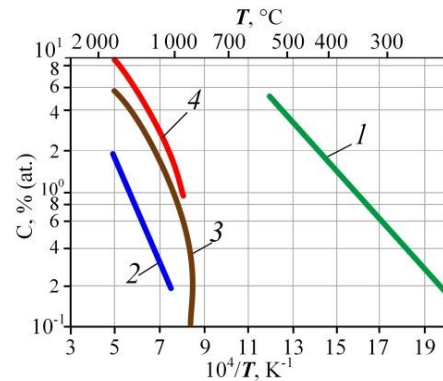


Fig. 5. Solubility limits of interstitial elements in zirconium [13]: 1 – $[H]_{\alpha-Zr}$; 2 – $[C]_{\alpha-Zr}$; 3 – $[N]_{\alpha-Zr}$; 4 – $[O]_{\beta-Zr}$.

After an operation in reactors, fuel-rod cladding has an oxide layer, which, in principle, can accumulate a

certain amount of hydrogen in its defects. In the work [14] it was noted that the standard methodology provides high-temperature isothermal out gassing of samples and allows determining only the total (volumetric) hydrogen content. However, it is important to know the distribution of the hydrogen content in the near surface layer. An experimental methodology that makes it possible to determine the amount of hydrogen in the oxide and metal phases of oxidized zirconium materials was proposed [15–18].

II. Effect of oxygen

Let us consider the thermodynamic prerequisites for the interaction of zirconium with oxygen. The main trend in the change of enthalpy with the penetration of oxygen into zirconium $\Delta H[O_2]_{\alpha}$ depending on the oxygen concentration is shown in fig. 6 [19].

In solid solutions of α -zirconium (O/Zr up to 0.2), the value of $\Delta H[O_2]_{\alpha}$ doesn't depend on the oxygen concentration and is 1194 kJ/molO₂. The absolute value of $\Delta H[O_2]_{\alpha}$ sharply decreases at O/Zr greater than 0.2. This is due to the ordering of oxygen atoms observed at low temperatures in the α -zirconium lattice.

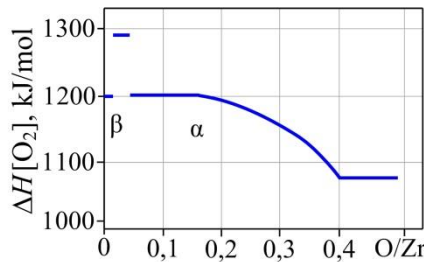


Fig. 6. Dependence of partial molar enthalpy of oxygen dissolution in zirconium $\Delta H[O_2]$ on oxygen concentration

$$\Delta G_{f,1/2-ZrO_2} = 4,1868 + (-130 + 0,022T)kJ/g - at. O \quad (3)$$

The high solubility of oxygen in zirconium alloys has the practical importance is in β -zirconium the solubility of oxygen is 10.4% at. (2% wt.) [24].

In α -zirconium the solubility of oxygen is even higher. There are values of the thermal solubility of oxygen in zirconium from 28.5 to 40% at. The most reliable is repeatedly confirmed value of $29 \pm 0.5\%$ at. ($6.75 \pm 0, 1\%$ wt.) at $T = 1900 \dots 2065^\circ\text{C}$. The limited solubility of oxygen ($[O]_{\alpha-Zr}$) depends slightly on temperature – at the phase boundary $\alpha/(\alpha + ZrO_2)$ $\ln(C_{0,sat})$ [% wt.] = 1.902 (regardless of temperature, the limited solubility of oxygen in α -zirconium is about 6.7% wt.) [25, 26]. The high solubility of oxygen in zirconium makes alloys of the Zr–O system very promising from the point of view of the practical use of bulk doping with oxygen as control method of the structure and properties of zirconium.

In the Zr–O system, there is only stable oxide ZrO₂, which has several modifications [27]. The low-temperature monoclinic modification ZrO₂ is resistant to 1205°C, where at this temperature transforms into a tetragonal one. The range of existence of ZrO₂ is from

[19].

For solid solutions, the enthalpy of their formation doesn't depend on temperature and its value can be calculated from equation 1 [20]:

$$\Delta H_{fo}[O]_{\alpha 298.15K} = -(585,3412 \pm 10,46), [kJ] \quad (1)$$

where f_o is the atomic content of oxygen ($f_o = O/Zr$).

The temperature dependence of the Gibbs free energy configuration of crystalline zirconium due to the dissolution with oxygen is shown in fig. 7 [21].

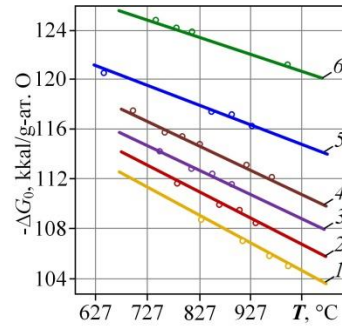


Fig. 7. Partial molar free energy of oxygen in Zr–O alloys depending on oxygen concentration in at. % [21]: 1 – 300, 2 – 250, 3 – 200, 4 – 150, 5 – 100, 6 – 50.

The temperature dependence of the Gibbs free energy configuration due to the dissolution of oxygen in liquid zirconium is described by equation 2 [22]:

$$\Delta G[O]_L = 4,1868 + (-111 + 0,021T)kJ/g - at. O \quad (2)$$

The temperature dependence of the Gibbs free energy during formation of zirconium oxide ($1/2 ZrO_2$) is described by equation 3 [23]:

temperature 1205 to $\sim 2347 \dots 2377^\circ\text{C}$. γ -ZrO_{2-x}, cubic modification, is formed starting from the eutectoid transformation temperature ($\sim 1402 \dots 1525^\circ\text{C}$) [20, 28, 29]. The low-temperature monoclinic modification ZrO₂ is resistant to 1205°C, where at this temperature transforms into a tetragonal one. Cubic γ -ZrO_{2-x} is stable up to a melting point of $\sim 2710^\circ\text{C}$. Polymorphism has great practical importance since it limits the use of pure oxide as a refractory material to the region of existence of a low-temperature modification. The cyclic temperature change in the region α -ZrO₂ \leftrightarrow β -ZrO₂ leads to cracking and destruction of the material [30]. In the cubic modification, eight oxygen atoms are located at a distance of 0.220 nm from the zirconium atoms. The tetragonal modification has two sets of distances, 0.2065 and 0.2455 nm, which correspond to compressed and elongated tetrahedra. In the structure of monoclinic ZrO₂, zirconium has a coordination number of 7 and there are two types of oxygen ions: with a coordination number of 3 and a coordination number of 4. Ions of the first kind O_i (CN₃) are in the same plane with three neighboring zirconium ions, the distance is 0.207 nm), the angles between bonds

are 104, 109 and 143°. Ions of the second type OII (coordination number 4) have surroundings in the form of a tetrahedron with an average distance of 0.221 nm. All angles between bonds, except for one (134°), lie in the range of 100...108°.

Lower oxides ZrO and Zr₂O₃ are formed at early stages of carbide reduction, and Zr₂O, ZrO, and Zr₂O₃ at early stages of oxide film growth [31]. ZrO monoxide has a cubic lattice of the NaCl type, the lattice parameter $a = 0.4584...0.464$ nm. These compounds are formed under special conditions. They don't determine the general patterns of behavior of the alloys of the system, and are of interest as examples of numerous metastable states. The probability of their formation, chemical composition and crystal structure are determined by the conditions of formation (the reason why the formation of a compound occurs not in equilibrium, but in metastable states). The range of such compounds is very wide and difficult to predict.

Solid solutions of oxygen in zirconium belong to the category of interstitial phases, i.e. solutions in which relatively small oxygen atoms (whose atomic radius is 0.066 nm) are located at interstices sublattices of Zr atoms (in α -Zr, the atomic radius is $R = 0.16$ nm) [27,32, 33]. In the α -zirconium lattice, oxygen atoms occupy octahedral positions. Octahedral interstices in the α -zirconium lattice have trigonal symmetry. The equilibrium pressure of oxygen in zirconium (p_{O_2}) is very low – $p_{O_2} \sim 1.01^{-65}$ Pa at a temperature of 450°C [24].

It is considered that if the oxygen concentration in the surface layer of the sample reaches 30% at. (~7% wt.), an oxide film of ZrO_{2-x} is formed. Oxygen ions diffuse through the film and, reaching the metal, increase its thickness (fig. 8) [34].

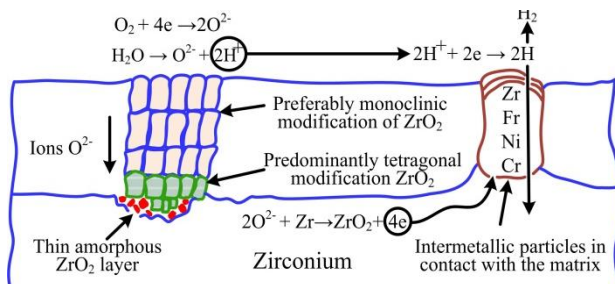


Fig. 8. Schematic representation of oxide film on Zr [34].

For example, the oxidation kinetics of zirconium alloys in aqueous solutions (close to operating conditions) is described by the function 3:

$$\Delta m = A \cdot t^n, \quad (4)$$

where Δm is the mass gain per unit area of the sample surface over time t ; A and n are constants.

In the initial period of an oxidation, the exponent n is 0.33...0.50. When the film thickness reaches 2...3 μm , there is a transition to linear oxidation (the "break" phenomenon) and $n = 1$.

Zirconium oxide ZrO₂ is polymorphic and, with increasing temperature, can exist in three crystalline modifications: monoclinic - α , tetragonal - β and cubic - γ (fig. 8). Oxide films with a thickness of more than 3 μm consist mainly of columnar crystals of ZrO₂, but often

contain inclusions of high-temperature modifications. The presence of such inclusions in zirconium oxides on Zr-1%Nb and Zr-2.5%Nb alloys after corrosion tests in an air, autoclaves and water vapor (including irradiation conditions) is confirmed. It is explained, as a rule, by the stabilizing effect of compressive stresses arising in the film due to the difference in the crystal lattice parameters of zirconium, ZrO₂ and oxides formed on inclusions of secondary phases. It is believed that the resulting stresses during the phase transformation Zr→ZrO₂ promote the crystallization of the initially amorphous oxide layer with the formation of metastable β - and γ -phases. As corrosion develops, the oxide-metal interface moves deep into the sample, and some of the formed metastable crystallites are located in the volume of the oxide. At a certain stage of oxidation, the level of compressive stresses in the outer layer of the film becomes insufficient to stabilize high-temperature modifications. It provides a martensitic transformation of the tetragonal and cubic phases into a monoclinic one. It is accompanied by an increase in volume and, as a result, by the formation of cracks and pores. The above mentioned scheme is considered as one of the most probable mechanisms of the "fracture".

An increase in the oxidation rate after a "fracture" is associated with a relatively easy penetration of the corrosive medium from the oxide surface due to its inappropriateness up to a thin layer. The last one is adjacent directly to the metal and plays the role of a diffusion barrier, limiting rate of corrosion processes. The linear kinetics of oxidation is explained by a constant equilibrium, when the rate of formation of inappropriateness in the oxide (that is, the rate of degradation of its protective properties) and the rate of formation of a new "barrier" become approximately the same. When passing through the "fracture", not only the oxidation kinetics of the material changes, but also the appearances of the oxide are occurred. Before the "fracture" the film is black, relatively dense and well-adhered to the metal surface. It determines its high protective properties. "Before the fracture", the films are deficient in oxygen: their composition corresponds to the formula ZrO_{2-x}, where $x < 0.5$. After the "break" the color of the film gradually changes from black to white. It is associated with a decrease in the number of anion vacancies and corresponds to approaching stoichiometric composition of ZrO₂, the protective properties of the film decrease: it becomes loose and crumbling.

Oxidized zirconium alloy consists of several layers: 1st – oxide; 2nd – metal adjacent to the ZrO oxide with increased oxygen content; 3rd - metal layer outside the oxygen diffusion zone. At a temperature of 300...500°C, up to 15% of the oxygen absorbed by the alloy during the oxidation process it is consumed to form a diffusion zone in the metal phase. Dissolving in the metal, oxygen can lead to coloring zirconium. It is known that zirconium materials containing more than 10% at. (2% wt.) of oxygen, incapable to plastic deformation. According to the experimental results, tests of the irradiated oxidized shell of nuclear fuel rod of BWR by an internal pressure of argon at $T = 325$ °C, the radial cracks appeared in the

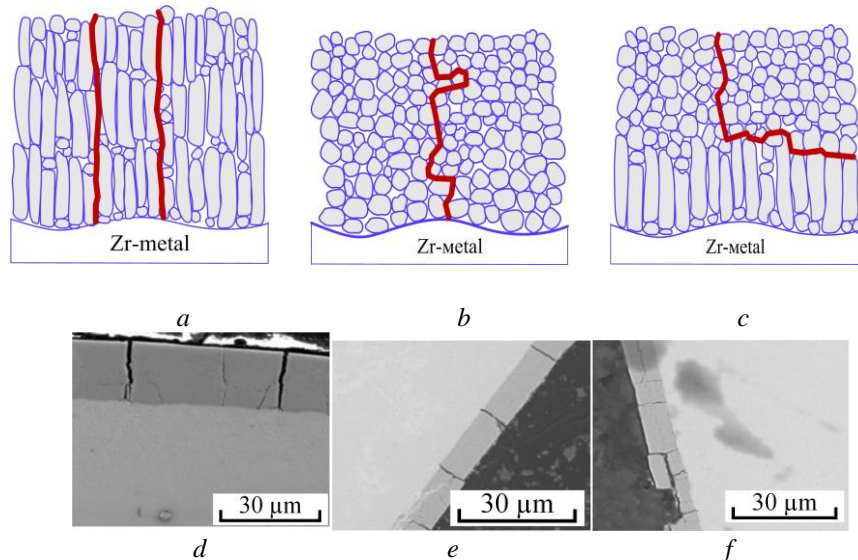


Fig. 9. Types of structures (*a, b, c*) and types of destruction (*d, e, f*) of oxide films of zirconium alloy samples [35]: *a, d* – mostly elongated, *b, e* – predominantly equilibrium, *f, c* – layered.

Zr(O) metal sublayer. It was brittle due to the presence of oxygen, continuing in the oxide phase, but not in the ductile metal.

An analysis of the microstructure of sample films allowed scientists [35] to distinguish three main types of characteristic grain structures of oxide films (fig. 9): with predominantly elongated grains, with predominantly equiaxed grains, and with a layered structure.

Most of the studied states are characterized by the structure of oxide films with predominantly elongated grains 400–500 nm long and 50–100 nm wide (fig. 9*a*). In such a film structure, individual equilibrium grains 30–40 nm in diameter are located between elongated grains. Their volume fraction in different states ranges from 10 to 30%.

The structure of a film with equiaxed grains (Fig. 9*b*) 30–40 nm in diameter was observed on samples of the E110G alloy after grinding by 2 μm. Such a structure contains a large number of pores up to 10 nm in diameter and microcracks 4.5 μm in length.

Layered film structures (type 3) (fig. 9*c*) are characteristic of samples of the E110G alloy after oxidation in water (state 1) and of the E125UMZ alloy after oxidation in steam. In such structures, elongated grains 60–80 nm thick are observed in the base metal substrate and equiaxed grains 20–30 nm in diameter are observed near the film surface.

Scientists J. Zhang, A. R. Oganov, X. Li, and others discovered the following thermodynamically stable compounds: Zr_6O , Zr_3O , Zr_2O , ZrO and ZrO_2 . They also established the Gibbs energies when the formation of the above mentioned compounds occurs (Fig. 10). Their calculations showed that the well-known monoclinic compound ZrO_2 exists in the widest range of chemical potentials in contrast to Zr_6O , Zr_3O , Zr_2O , and ZrO , which are stable only under highly reducing conditions [36].

It was established that when oxygen penetrates into zirconium the formation of ordered suboxides is possible [37].

In [38], a positive effect of oxygen on fatigue life was recorded both at room temperature and at elevated one ($T = 350^\circ\text{C}$) (fig. 12). The positive effect of oxygen on the

fatigue life of zirconium was also recorded by other researchers. The probable reason for such a positive effect of oxygen on the fatigue life of zirconium is attributed by the authors to the formation of a solid solution of the interstitial elements in the metal matrix.

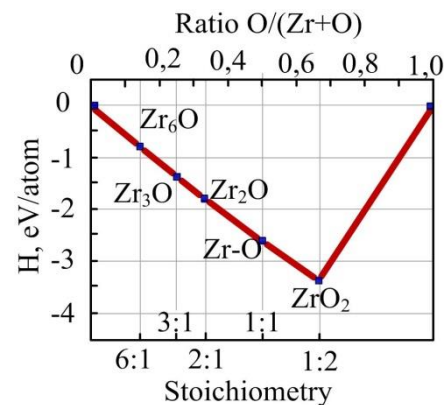


Fig. 10. Enthalpy of formation of zirconium oxides [36].

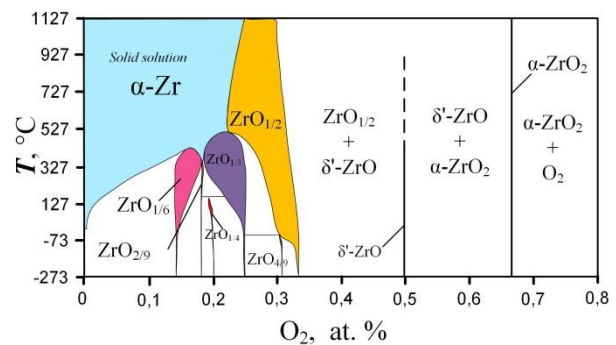


Fig. 11. Calculated phase diagram of ZrO_x [37]. (Colored areas indicate single-phase regions, not filled areas indicate two-phase regions).

The authors of the work note that with an increase in the oxygen content the grain size decreases (fig. 13): at 140 ppm O_2 it is 19 μm, at 660 ppm O_2 it is 15 μm, and at 1740 ppm O_2 it is 13 μm [38].

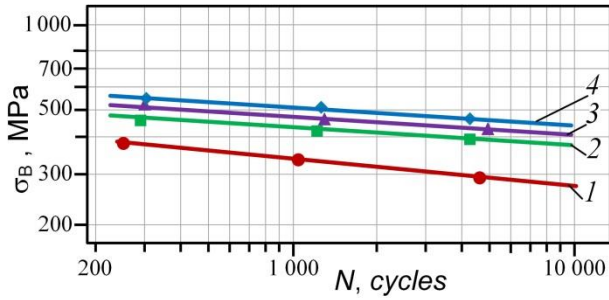


Fig. 12. Fatigue curves of zirconium alloy samples in an air at $T = 350^\circ\text{C}$ with different oxygen contents (ppm): 1 – 140, 2 – 660, 3 – 1200, 4 – 1740 [38].

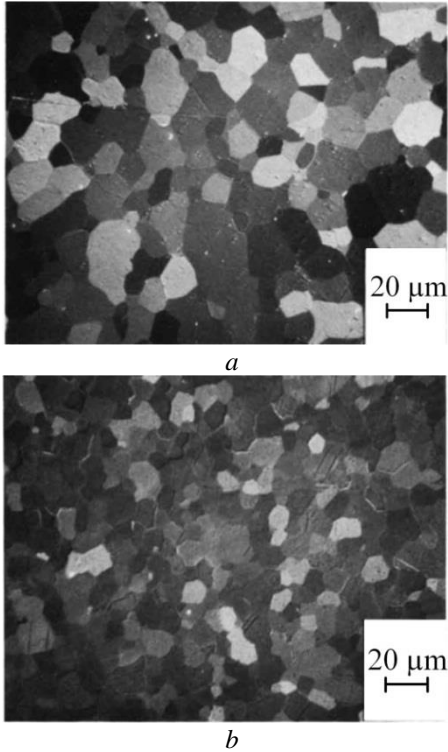


Fig. 13. Microstructure of zirconium with different oxygen content: a – 140 ppm, b – 1200 ppm [38]

According to [39], oxygen affects the ductile-brittle transition in zirconium alloys (Fig. 14) and it is determined as a function of oxygen concentration and temperature.

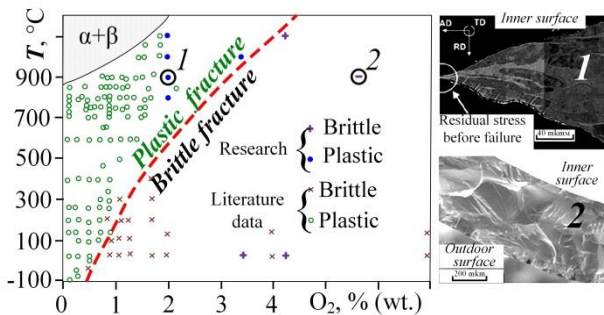


Fig. 14. Ductile-brittle transition in zirconium alloys as a function of oxygen concentration and temperature [39].

In [40], the fracture surfaces of E110 and E125 zirconium alloys with an oxygen content of

0.003...0.004% wt. and 0.007...0.008% wt., respectively, were analyzed. The authors note that the fracture surface of an alloy with high oxygen content contains a large number of fatigue grooves, which indicates high fracture energy intensity. Also in [40], the durability of low-cycle bending of zirconium-based alloys with different oxygen content (0.003...0.004% wt. and 0.007...0.008% wt.) is shown. In particular, it was shown that an alloy with lower oxygen content has greater durability, both at a room temperature and at a temperature of 350°C .

It was pointed out in [41] that an increase in the oxygen content leads to a decrease in the twinning process and the onset of micropore nucleation already at the late stages of uniform plastic deformation.

It was shown [6] that an increase in the oxygen content in clad pipes made of Zr-1%Nb alloy, causing intense hardening (an increase in the yield strength and ultimate strength of pipes made of Zr-1%Nb alloy in the axial direction is 15.45 MPa) for every 0.01% wt. O_2 , which is 27.6 kg/mm² for each % at. oxygen), does not lead to a significant loss of plasticity (the intensity of the loss of plasticity of pipes in the axial direction does not exceed 2% for every 0.01% wt. O_2) [6].

It should be noted that the solubility of the interstitial elements in zirconium depends on the other interstitial elements already presented in the metal. For example, the solubility of hydrogen in α -zirconium depends on the dissolved oxygen in the metal matrix. The solubility of hydrogen in the Zr(O) solid solution can be estimated using triple Zr-O-H diagram (Fig. 15). At a low oxygen content (0...15% at.), the solubility of hydrogen in the α -phase increases, and then, at an oxygen content of 15...28% it decreases [42].

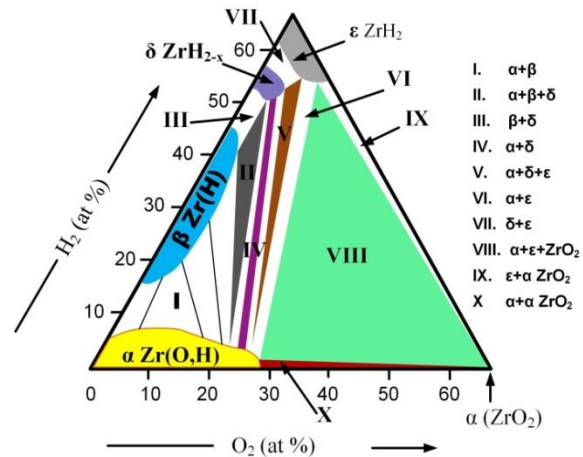


Fig. 15. Ternary system “Zr-O-H” at a temperature $T = 700^\circ\text{C}$ [42].

For thin brittle coatings covering ductile substrate the expected trend in the development of oxide damage during deformation is shown in Fig. 16 [43]. The density of oxide cracks increases with applied strain and reaches saturation at large plastic strains. Cracks parallel to the applied load appear after saturation in the cross-linking phase, and at very high strain, the brittle layer breaks off. The peel strain of the oxide layer will depend on the strength of the oxide-Zircaloy-4 bond as well as on the crack density.

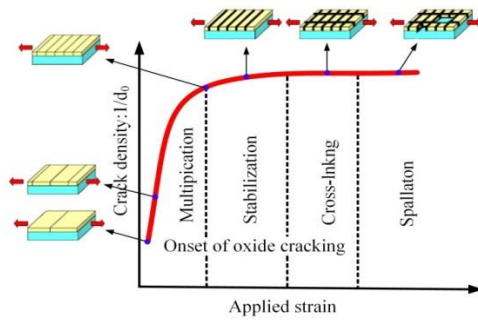


Fig. 16. Schematic representation of oxide damage depending on applied deformations [43].

The initial “air” oxide is dense and protective and it is presented on all surfaces of the Zr alloy exposed to an oxygen-containing environment; it consists of very small equiaxed ZrO_2 nanocrystals with a certain orientation relative to the orientation of the Zr grains where they are formed (Fig. 17) [44]. Some of these grains with a preferred orientation will grow into columnar grains about 2 μm in size. Preferred crystallite orientations are those that minimize stress due to volume change from Zr to ZrO_2 (Pilling-Bedworth ratio ~ 1.565). According to [44], small discrepancies in the orientation of crystals relative to the preferred orientation cause the accumulation of stresses. Estimated, the highest compressive stresses of about 1200 MPa are presented near the metal/oxide interface and near

zero near the outer surface in the 80 μm thick oxide layer formed on the ZIRLO alloy [44].

A significant number of works [1, 45-50] is devoted to the study of the oxygen effect on the characteristics of zirconium alloys and the behavior of the material under irradiation. It was established that the segregation of the interstitial impurities increases the risk of failure during operation [37]. On the other hand, due to its hardening effect, oxygen promotes an increase in the long-term strength and creep resistance of Zr alloys under irradiation [46, 47]. Therefore, oxygen is introduced into the composition of the Zr-1%Nb alloy as an alloying element up to 0.14% or more [1]. It was shown in [1] that an increase in the oxygen content in clad pipes made of the Zr-1% Nb alloy to 0.16%, causing an intense hardening, does not lead to a significant loss of plasticity. In addition, with an increase in the temperature of mechanical tests, oxygen hardening weakens. The presence of oxygen up to 0.5% with its uniform distribution does not lead to a significant decrease in the corrosion resistance of zirconium-niobium alloys [41, 50].

It was established [41] that for deformed samples with an oxygen content of 0.06...0.08%, the presence of a large number of twins in the fracture zone is typical (Fig. 18, a). However, with an increase in the oxygen content, their number decreases with distance from the fracture site (Fig. 18, b). In samples with an oxygen content of 0.11%, twins

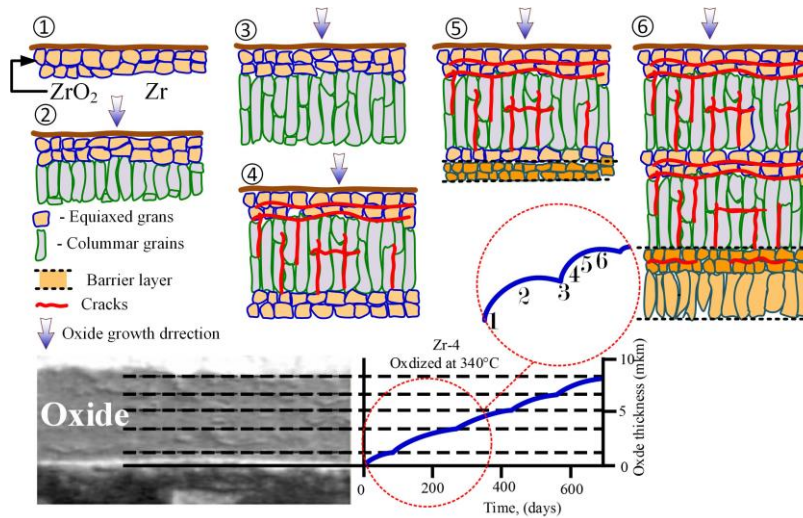


Fig.17. Relationship between schematic oxide structure and oxidation kinetics. Corrosion of Zry-4 alloy in an autoclave at temperatures of 340-360°C [44].

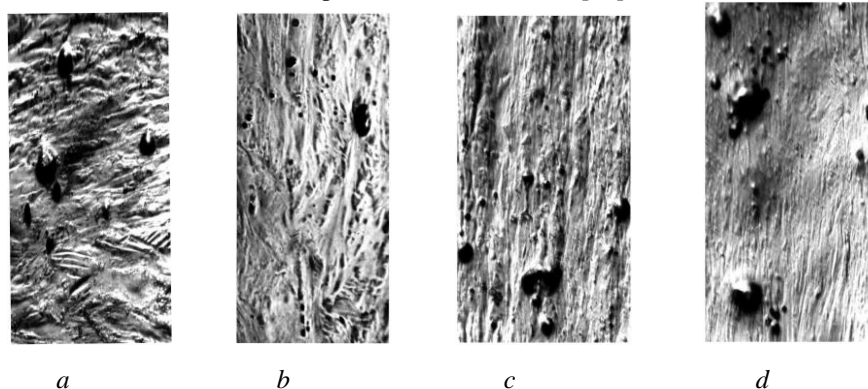


Fig.18. Structure of samples of hot-worked pipes with different oxygen content in the fracture zone, $\times 500$:
a – 0.06% O_2 ; *b* – 0.08% O_2 ; *c* – 0.11% O_2 ; *d* – 0.18% O_2 [41].

are rarely found even near the fracture zone (Fig. 18, c), and in deformed samples with 0.18% oxygen no twins were detected by light microscopy (Fig. 18, d). The scientists concluded that an increase in the amount of oxygen leads to the suppression of twinning processes and an increase in the probability of the formation of irreversible structural defects at lower degrees of deformation.

According to [6], it follows that, being in a solid solution, oxygen both in pure zirconium and zirconium based alloys causes hardening at a room temperature equal to (18 ± 4) MPa for every 0.01% wt. O_2 , (30 ± 5) kg/mm² each 1.0% at. oxygen. Oxygen hardening weakens (the value of $\sigma_T/\Delta C_O$ decreases) with an increase in the oxygen content and an increase in the temperature of mechanical tests.

The presence of oxygen in zirconium has a strong effect on the behavior of vacancies, their mobility and thermal stability. The results of studies of the growth rate of dislocation loops under electron irradiation (studies in dynamics under irradiation in a high-voltage electron microscope), carried out by Helio and coworkers on zirconium with different oxygen contents [10], showed that the migration energy of vacancies increases significantly with increasing content oxygen (0.72 eV for pure zirconium to 1.58 eV for 1760 ppm O_2).

Thus, the effect of oxygen on the properties is ambiguous and requires an additional research in each specific case.

III. Effect of nitrogen

The reaction of zirconium alloys with nitrogen is very slow. Pre-oxidized zirconium alloys react ten times faster with nitrogen, and pre-oxidized and homogenized lining, i.e. α -Zr(O) stabilized by the oxygen atom reacts almost two orders of magnitude faster. As a rule, zirconium nitride appears when there is no oxygen in the gas phase and is in a solid solution (fig. 20) [52]. These conditions are locally established at the metal-oxide interface or can exist globally under conditions of lack of oxygen. An oxidation with oxygen and steam has a parabolic kinetics at temperatures exceeding 1050 °C, and at lower temperatures it first becomes parabolic before proceeding to rupture. A mixture of steam or oxygen with nitrogen accelerates degradation due to the formation and re-oxidation of zirconium nitride, resulting in a cellular and non-protective oxide/nitride. The porous oxide and vapor in the atmosphere lead to a strong absorption of hydrogen by the residual metal [52].

It was established that the consequences of the high-

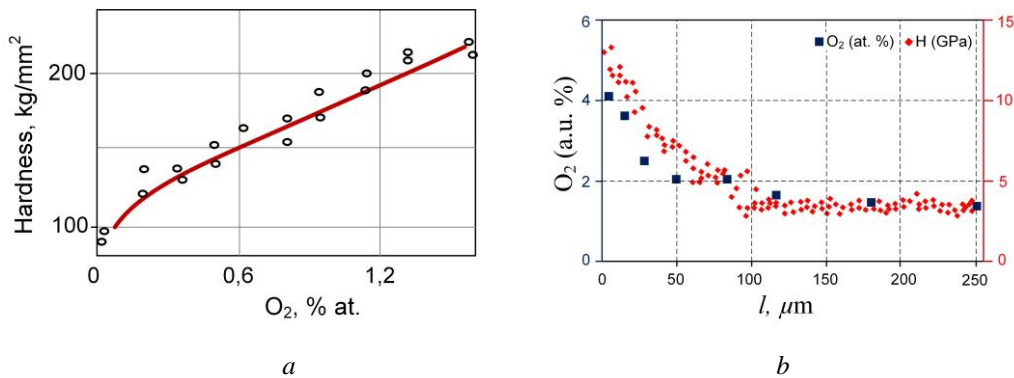


Fig. 19. Influence of oxygen content on zirconium hardness (a) and hardness distribution over the cross section (b) [38].

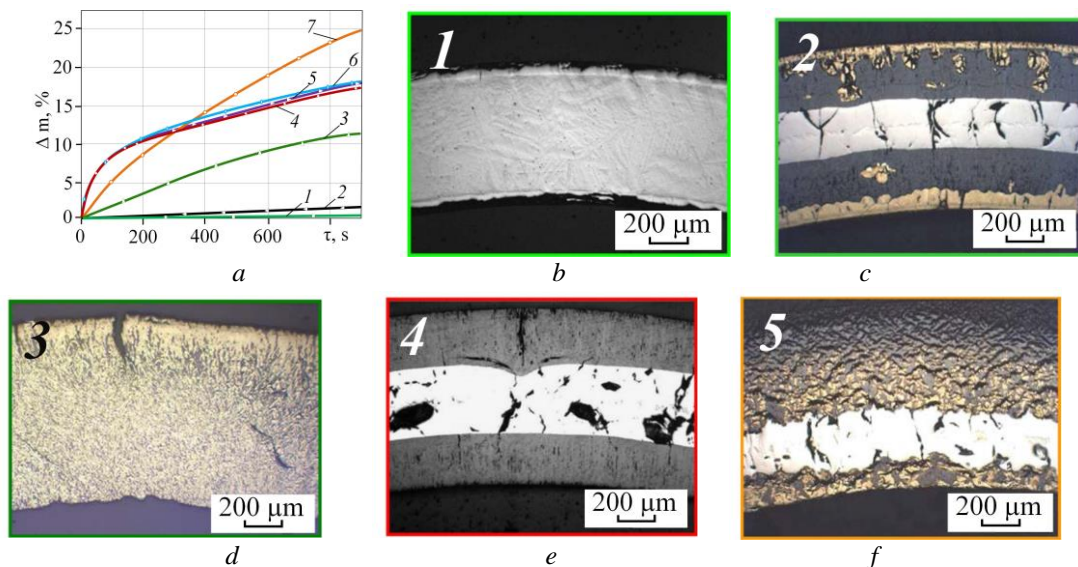


Fig. 20. Weight gain (a) and structure of fuel rod tubes (b, c, d, e, f) after treatment in various media at $T = 1200^\circ\text{C}$ [53]: 1, b – N_2 ; 2, c – O_2+N_2 ; 3, d – α -Zr(O)+ N_2 ; 4, e – O_2 ; 5 – O_2 +air; 6 – H_2O ; 7, f – air [52].

temperature interaction of zirconium with nitrogen and water vapor significantly depend on the proportions of these components. In particular, it was shown that at a temperature of 800°C the greatest destructive effect will take place at 90% N₂ and 10% H₂O (fig. 21) [53], which correlates with weight gain.

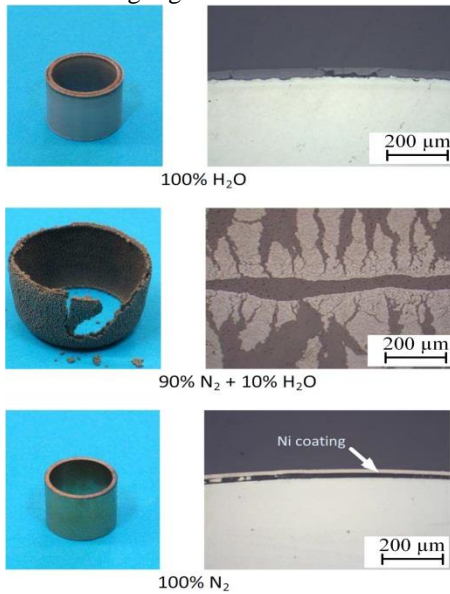


Fig. 21. Appearance after tests and photomicrographs of selected samples of Zircaloy-4 after 6 hours of oxidation at 800°C in various gas compositions [53].

The dissolution of nitrogen in the zirconium matrix has a significant effect on plasticity and strength: with an increase in the content of the interstitial elements plasticity decreases, while strength increases [11].

IV. Effect of nitrogen-oxygen mixture

Recently, according to literary sources, much attention has been paid to the study of the mechanism of interaction of air (in fact, the simultaneous action of oxygen and nitrogen) with zirconium cladding pipes. Works in this direction were intensified after the accident at the Fukushima nuclear power plant. According to an analysis of the consequences of the accident at this nuclear power plant, it is quite possible that a critical situation may arise when the supply of cooling water stops and the fuel claddings experience a significant increase in temperature in a short time period. From the point of view of safety, the performance of fuel rod cladding at high temperatures is deteriorated more rapidly in an air than in a vapour. In particular, scientists showed that zirconium nitride is formed only in the absence of oxygen in the gas phase and in the presence of oxygen in the metal phase [54].

Using the p_{O_2}/p_{N_2} diagram (fig. 22), we can determine the stability limits of the existence of Zr, ZrO₂ and ZrN depending on a temperature [55]. For example, at a temperature $T = 927^\circ\text{C}$ zirconium nitride ZrN is stable at a very low partial pressure of oxygen ($p_{O_2} < 10^{-32}\text{Pa}$) and at a partial pressure of nitrogen not exceeding 10^{-17}Pa .

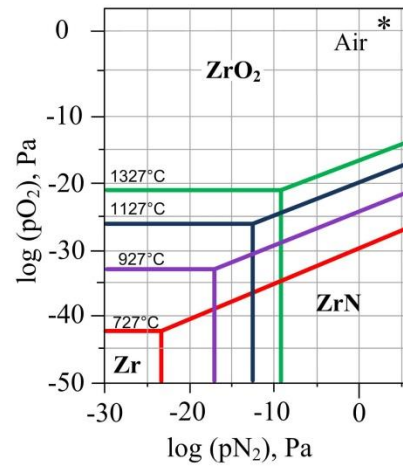


Fig. 22. Diagram of p_{O_2}/p_{N_2} stability [55]. (Note: The star in the upper right corner represents the composition of an air).

The oxygen content in the metal has a significant effect on the weight gain and structure of zirconium samples at a temperature $T = 1100^\circ\text{C}$ (fig. 23). According to the research results of scientists [55], the weight gain of the nitrated sample increases with an increase in the oxygen content in the metal.

Baldwin et al. [55] studied in a detail the phenomena observed when the nitrogen content in gas mixtures with oxygen changes. The microstructure of the layer changes significantly when the nitrogen content in the mixture changes from 0 to 100%.

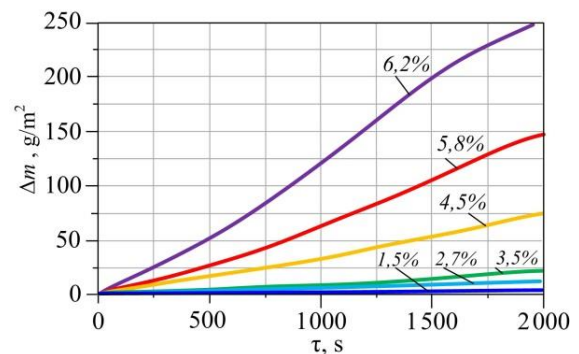


Fig. 23. Weight gain of samples with different oxygen content during nitriding at $T = 1100^\circ\text{C}$ [55].

In pure oxygen at $T = 900^\circ\text{C}$ the degradation of the oxide layer on zirconium somewhat slows down. In a layer containing up to 15% N₂ the isolated ZrN particles (yellow) appear, but the oxide bases of the layer is still subject to degradation. At nitrogen concentration above 15% a continuous ZrN film adjacent to the metal is revealed, and a general deformation of the initial zirconium sample is observed. At the same time, local penetrations of the oxide into the base disappear. Finally, only in an atmosphere of pure nitrogen oxide completely disappears from the system, only a continuous ZrN film is observed, and oxide degradation and deformation of the base do not appear [55].

Fig. 24 shows a diagram illustrating structure of an oxide layer formed on zirconium as a result of its successive heating in different gases at $T = 900^\circ\text{C}$ [56].

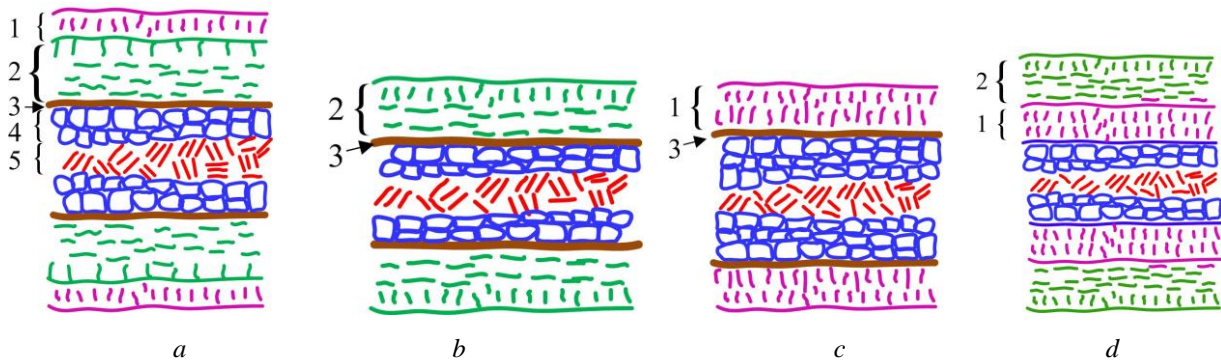


Fig. 24. Scheme of structure of near-surface layer formed on zirconium as a result of successive heating at $T = 900^{\circ}\text{C}$ in various gaseous media [56]: *a* – oxygen \rightarrow air; *b* – nitrogen \rightarrow air; *c* – oxygen \rightarrow nitrogen; *d* – air \rightarrow oxygen; 1 – ZrO_2 formed in O_2 ; 2 – ZrO_2 formed in air; 3 – ZrN ; 4 – $\alpha\text{-Zr}$; 5 – $\beta\text{-Zr}$.

Figure 24 illustrates the following:

a) during secondary heating in a nitrogen-enriched gas environment a continuous ZrN film is always observed on the metal after scale degradation;

b) upon secondary heating in an oxygen, the ZrN film (previously formed in an air or in nitrogen) more or less quickly disappears; a zirconium plate can even quickly burn out if the primary scale consisted only of ZrN ;

c) during secondary heating in an oxygen or in an air on the sample the scale formed as a result of the first heating always forms the outer zone of the final oxide layer.

Therefore, an oxidation occurs due to diffusion of oxygen to the metal-oxide interface, while the black oxide film may become white if it moves away from this interface, however, the internal scale zone formed as a result of secondary oxidation may be a continuous black layer.

Scientists J. Birchley and L. Fernandez-Moguel from the Institute. P. Scherrer (Switzerland) [57] established some patterns of saturation of the Zry-4 zirconium alloy after treatment in various gaseous media. In particular, it was shown that the largest increase in the mass of this alloy is observed after treatment in an air, and the smallest one after the treatment in pure nitrogen (fig. 25).

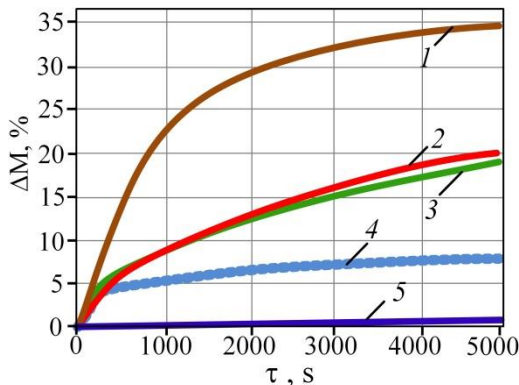


Fig. 25. Weight gain of Zry-4 zirconium alloy after treatment at $T = 1100^{\circ}\text{C}$ in various gaseous media [57]: 1 – air; 2 – $\text{O}_2 \rightarrow$ air; 3 – O_2 ; 4 – $\text{O}_2 \rightarrow \text{N}_2$; 5 – N_2 .

The dissolution of both nitrogen and oxygen in the zirconium matrix has a significant effect on plasticity and

strength: with an increase in the content of the interstitial elements plasticity decreases, and strength increases (fig. 26) [11].

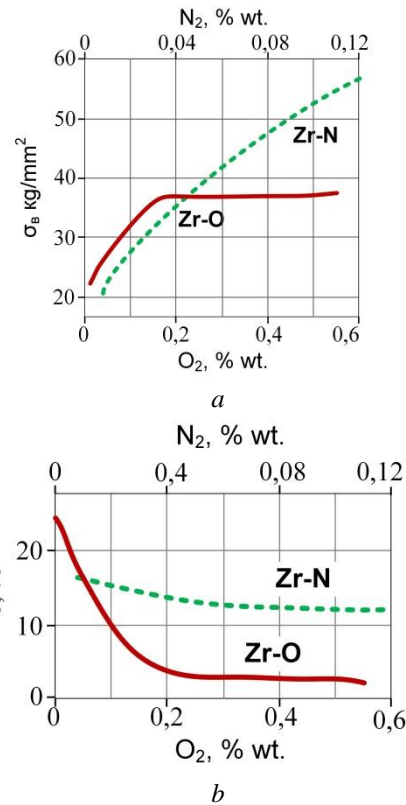


Fig. 26. The effect of oxygen and nitrogen on strength (a) and elongation (b) of zirconium [11].

It was established that the interaction of nitrogen with zirconium can lead to the existence of several thermodynamically stable compounds (Fig. 21) ZrN , Zr_2N , Zr_4N_3 , Zr_6N_5 , Zr_8N_7 , $\text{Zr}_{15}\text{N}_{16}$, Zr_7N_8 and Zr_4N_5 [58]. It can be assumed that in the presence of such ordered compounds, a positive effect on the physicomaterial properties of the metal can be achieved, in particular, using hydrogenation of oxidized or nitrided zirconium alloys.

Table 1

Characteristics of zirconium oxynitrides [59].

| № | ZrN _z O _y | | | Crystal lattice parameter, nm | Density, kg/m ³ | Phase composition |
|----|---------------------------------|------|-------|-------------------------------|----------------------------|--|
| | z | y | z + y | | | |
| 1 | 0,71 | 0,32 | 1,03 | 0,4576 | 6910 | ZrN _z O _y |
| 2 | 0,83 | 0,20 | 1,03 | 0,4576 | 6950 | |
| 3 | 0,81 | 0,21 | 1,02 | 0,4575 | 6940 | |
| 4 | 0,76 | 0,19 | 0,95 | 0,4576 | 6940 | |
| 5 | 0,80 | 0,10 | 0,90 | 0,4574 | 6960 | |
| 6 | 0,76 | 0,09 | 0,85 | 0,4576 | 6940 | |
| 7 | 0,57 | 0,29 | 0,86 | 0,4574 | 6830 | |
| 8 | 0,50 | 0,30 | 0,80 | 0,4575 | 6,82 | |
| 9 | 0,67 | 0,38 | 1,03 | 0,4576 | – | |
| 10 | 0,65 | 0,38 | 1,03 | 0,4576 | – | ZrN _z O _y , ZrO ₂ , |
| 11 | 0,48 | 0,56 | 1,04 | 0,4574 | – | α-ZrN _z O _y |

V. Prerequisites for formation of zirconium oxynitrides

The characteristics of a number of zirconium oxynitrides were formed and studied [59] (Table 1).

The authors indicated that bracketed mixtures of the initial components (ZrO₂, Zr, oxynitrides ZrN_{0,76}O_{0,14} and ZrN_{0,87}O_{0,12}) were sintered in a vacuum (~10 Pa) at a temperature of $T = 1500^{\circ}\text{C}$ for 50 h.

The authors [59] noted that ZrN_zO_y oxynitride has a structure of the NaCl type. They also showed that ZrO₂ and ZrN_zO_y can be detected by X-ray diffraction if their minimum content in samples reaches 3...4% wt. The same work presents a schematic isothermal section (1500°C) of the Zr–N–O phase diagram (fig. 27). The formula ZrN_{0,72}O_{0,31} corresponds to a single-phase case with a maximum oxygen content. The composition of ZrN_{0,65}O_{0,36} has already turned out to be two-phase. These results agree with the concept of the maximum solubility of oxygen not only in carbide, but also in zirconium nitride. The X-ray diffraction patterns of the experimental samples indicated the presence of a hexagonal α-ZrN_zO_y solid solution along with the ZrN_zO_y and ZrO₂ phases. Its lattice periods, for example, for the composition ZrN_{0,1}O_{0,92} were $a = 0.3244$ nm, $c = 0.5372$ nm and differed markedly from the existing pure metal ($a = 0.3233$ nm, $c = 0.5146$ nm).

When studying interaction of ZrO₂ with ammonia ($T = 950^{\circ}\text{C}$), the authors revealed a number of metastable zirconium oxynitrides with complex structures that are stable at formation temperatures in a nitrogen medium. They corresponded to the compositions Zr₂ON₂ ($a = 1.0135$ nm), Zr₇O₈N₄ ($a = 0.6246$ nm, $\alpha = 99^{\circ}35'$), and Zr₇O₁₁N₂ (rhombohedral cell). When heated in an inert atmosphere, all of these oxynitrides decomposed with the formation of ZrO₂ dioxide and ZrN cubic nitride. Under the conditions of high-temperature vacuum sintering, the formation of oxynitrides Zr₂ON₂, Zr₇O₈N₄, Zr₇O₁₁N₂ was not observed (fig. 27).

Van Lam Do et al. [60] determined the phase

boundaries in the Zr–N–O system at $T = 1100^{\circ}\text{C}$. As noted by these authors, the limit of oxygen solubility in Zr(N, O)_{1-x} is larger than the limit determined by Zanulin [61]. It is interesting to note that the stability domain of Zr(N, O)_{1-x} indicates a hypothetical zirconium monoxide ZrO. Fig. 28 also shows the stability region of the Zr hexagonal phase, which is broadened when both nitrogen and oxygen are dissolved. Monoclinic ZrO₂ is in equilibrium with Zr(N, O)_{1-x}, forming ZrO₂+Zr(N, O)_{1-x} and a two-phase region.

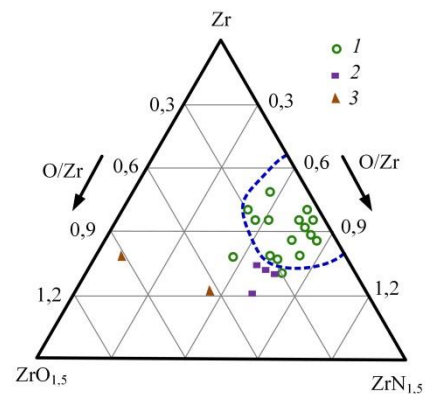


Fig. 27. Phase composition of samples of Zr–N–O system at 1500°C [59]: 1 – single-phase, 2 – two-phase, 3 – three-phase.

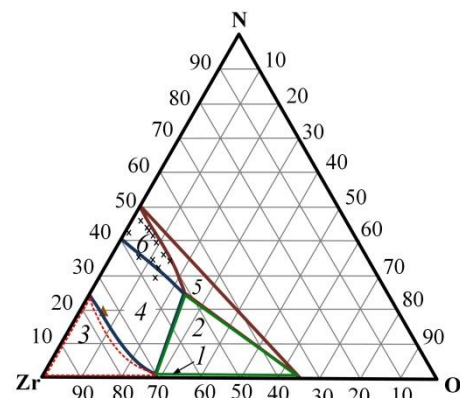


Fig. 28. Phase limits in Zr–N–O system at 1100°C: 1 – α-Zr+ZrO₂; 2 – α-Zr+Zr(N, O)_{1-x}+ZrO₂; 3 – α-Zr; 4 – α-Zr(N, O)_{1-x}; 5 – ZrO₂+Zr(N, O)_{1-x}; 6 – Zr(N, O)_{1-x} [60].

The three system has not yet been comprehensively studied. The phase composition in quenched zirconium samples partially burned in an air was determined. The results of this study are shown in fig. 29 [62]. Samples of metallic Zr partially reacted with an air at a combustion temperature of 2400°C. In addition to the ZrO_2 - $ZrN_{4/3}$ oxynitride phases, Zr-rich inclusions with compositions that diffuse between ZrN and $ZrO_{0.25}$ were reported. The nature of these inclusions was not further specified. The aim of this study is to further study the existing phases and melting ratios in the Zr-O-N ternary system. Samples with a certain composition were subjected to laser heating until a melt formed.

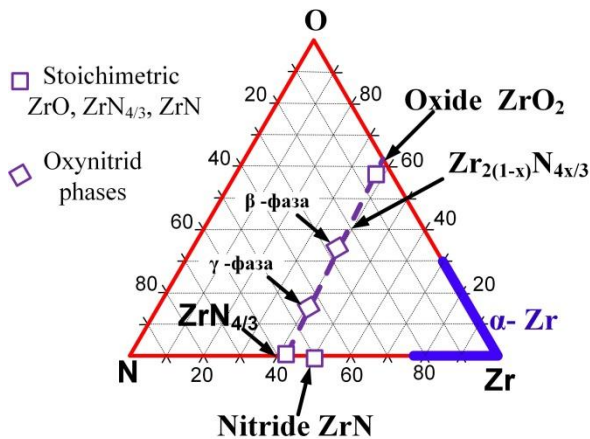


Fig. 29. Phase compositions in quenched samples during combustion of Zr in an air [62].

It should also be noted, that for many years researchers successfully used thermochemical treatment in a controlled oxygen or nitrogen-containing gas environment to improve functional properties such as oxidation resistance [63], long-term strength [64] of zirconium alloys, and a set of mechanical properties [65, 66], tribological properties [67] of oxidized titanium alloys.

Conclusions

Summing up literature review on the effect of the

content of the interstitial elements (in particular, oxygen, nitrogen, hydrogen) on a number of functional properties of zirconium alloys, the following conclusions can be drawn:

- in the scientific and technical literature, the main attention is paid to the bulk alloying of zirconium alloys with oxygen and nitrogen, their testing at high temperatures;
- it was shown that the interstitial elements (oxygen, nitrogen) have different limiting solubility's in zirconium;
- it was studied that, depending on the content of oxygen or nitrogen, they will either dissolve or form chemical compounds;
- it was confirmed that nitrogen and oxygen form a number of stable compounds of suboxides and subnitrides, which can improve the properties of zirconium;
- it was shown that the presence of oxide and nitride layers effect the properties of zirconium alloys;
- the results of the influence of treatment in a media containing both oxygen and nitrogen components on the properties of zirconium are given;
- thermodynamic prerequisites for the formation of zirconium oxynitrides of different phase composition in a nitrogen-oxygen gas mixture are shown.

Trush V.S. – Ph.D, senior research fellow, doctoral student;
Pylypenko N.N. – doctor of technical sciences, senior research fellow, head of the department of pure metals, metal physics and technologies of new materials;
Stoev P.I. – doctor of physics-mathematics, professor, leading research fellow;
Tikhonovsky M.A. – Ph.D, head of Research Laboratory of Electrophysical Materials and Technical Superconductor;
Pohrelyuk I.M. – doctor of technical sciences, professor, head of Department of Material Stage Bass of Surfing Engineering;
Fedirko V.M. – doctor of technical sciences, professor, chief research fellow;
Lukyanenko A.G. – Ph.D, senior research fellow;
Lavrys S.M. – Ph.D, research fellow.

- [1] A.S. Zaimovsky, A.V. Nikulina, N.G. Reshetnikov, Zirconium alloys in the nuclear industry, Energoizdat, Moscow, (1981). (in Russian).
- [2] C. Lemaignan, Zirconium Alloys: Properties and Characteristics, *Comprehensive Nuclear Materials* 217–232 (2012); <https://doi.org/10.1016/b978-0-08-056033-5.00015-x>
- [3] N.A. Azarenkov, L.A. Bulavin, I.I. Zalyubovsky, V.G. Kirichenko, I.M. Neklyudov, B.A. Shilyaev, Nuclear energy. Chapter 2. Nuclear power. Textbook, V.N. Karazin KhNU, Kharkiv, (2012). (in Russian).
- [4] E.O. Adamov, Yu.G. Dragunov, V.V. Orlov et al. Mechanical engineering of nuclear technology. T. IV-25. In 2 books. Book. 1, Mashinostroenie, Moscow, (2005). (in Russian).
- [5] T.P. Chernyaeva, A.I. Stukalov, V.M. Gritsina, Oxygen in zirconium: A review based on the materials of domestic and foreign publications for 1955-1999. Scientific-technical complex "Nuclear fuel cycle", NNTs KIPT, Kharkiv, (1999). (in Russian).
- [6] T.P. Chernyaeva, A.I. Stukalov, V.M. Gritsina, Influence of oxygen on mechanical properties of zirconium, *Problems of atomic science and technology* 12(1), 96-102 (2002). (in Russian).
- [7] C. Anghel. Modified oxygen and hydrogen transport in Zr-based oxides. Doctoral Thesis. Division of Corrosion Science Department of Materials Science and Engineering Royal Institute of Technology. Stockholm, Sweden, 256 (2006); <https://www.diva-portal.org/smash/get/diva2:10706/FULLTEXT01.pdf>.

- [8] L. Gribaudo, D. Arias, J. Abriata, The N-Zr (Nitrogen-Zirconium) System. *Journal of Phase Equilibria*, 15(4), 441-449 (1994); <https://doi.org/10.1007/bf02647575>.
- [9] C. Lemaignan, A. T. Motta, Zirconium Alloys in Nuclear Applications. *Materials Science and Technology* (2006). <https://doi.org/10.1002/9783527603978.mst0111>.
- [10] T.P. Chernyaeva, A.I. Stukalov, V.M. Gritsina, Oxygen behavior in zirconium, *Problems of atomic science and technology* 2(77), 71-85 (2000). (in Russian).
- [11] D. Douglas, Metal science of zirconium. Atomizdat, Moscow, (1975). (in Russian).
- [12] I. Kogan., B.A. Kolachev, Yu.V. Levinsky et al. Constants of interaction of metals with gases. Metallurgiya, Moscow, (1987). (in Russian).
- [13] V.M. Azhazha, P.N. Vyugov, S.D. Lavrinenko, V.I. Lapshin, N.N. Pilipenko, Electron beam melting of zirconium, *Problems of atomic science and technology* 5, 3-11 (2000). (in Russian).
- [14] F. Groeschel, A. Hermann, Experiments to understand the corrosion process of fuel rod claddings. Annual Rep. PSI, Annex IV. Villigen, Switzerland, (1996).
- [15] A. Shmakov and el. Separate determination of hydrogen in zirconium alloys and in their oxide. PSI TM-43-97-03. Villigen, Switzerland, (1997).
- [16] H. Bruchertseifer et ell. Investigation of hydrogen distribution in oxidised zirconium alloys by thermo-release method. Proc. annual meeting on Nucl. Technology «Jahrestagung Kerntechnik», München, Germany (1998).
- [17] A.A. Shmakov, E.A. Smirnov, and Kh. Bruchertzeufer, Hydrogen Distribution and Diffusion in Oxidized Zirconium-Based Alloys, *Atomic Energy* 85(3), 253-255 (1998) (in Russian).
- [18] A.A. Shmakov, Diffusion of hydrogen in zirconium oxides before and after the “break”. *Problems of atomic science and technology*. Issue. 1, 362-365 (2006) (in Russian).
- [19] G. Boureau, P. Gerdanian, High temperature thermodynamics of solutions of oxygen in zirconium and hafnium, *Journal of Physics and Chemistry of Solids* 45(2), 141-145 (1984); [https://doi.org/10.1016/0022-3697\(84\)90112-4](https://doi.org/10.1016/0022-3697(84)90112-4).
- [20] P.Y. Chevalier, E. Fischer, Thermodynamic modeling of the O-U-Zr system, *J. Nucl. Mater.* 257(3), 213-255 (1998); [https://doi.org/10.1016/s0022-3115\(98\)00450-4](https://doi.org/10.1016/s0022-3115(98)00450-4).
- [21] K.L. Komarek, M. Silver, Thermodynamics of Nuclear Materials: Proc. Int. Conf. IAEA, Vienna, p. 749-774 (1962).
- [22] D.R., Olander, W.-E. Wang, Thermodynamics of U-O and Zr – systems and application to analysis of fuel liquefaction during severe accidents in light water reactors, *J. Nucl. Mater.* 247, 258-264 (1997); [https://doi.org/10.1016/s0022-3115\(97\)00052-4](https://doi.org/10.1016/s0022-3115(97)00052-4).
- [23] M.V. Ganduglia-Pirovano, A. Hofmann, Oxygen vacancies in transition metal and rare earth oxides: Current state of understanding and remaining challenges, *J. Sauer. Surface Science Reports* 62, 219-270 (2007); <http://www2.hu-berlin.de/chemie/sfb546/Publikationen2008/fullpapers/C5/GHS07.pdf>.
- [24] T. Tsuji, M. Amaya, Study on order-disorder transition of Zr-O alloys (O/Zr = 0 - 0.31) by heat capacity measurement. *J. Nucl. Mater.*, 223(1), 33-39 (1995); [https://doi.org/10.1016/0022-3115\(95\)00019-4](https://doi.org/10.1016/0022-3115(95)00019-4).
- [25] O.M. Sreedharan, J.B. Gnanamoorthy, Oxygen potentials in alkali metals and oxygen distribution coefficients between alkali and structural metals - an assessment. *J. Nucl. Mater.*, 89(1), 113-128 (1980); [https://doi.org/10.1016/0022-3115\(80\)90015-x](https://doi.org/10.1016/0022-3115(80)90015-x).
- [26] D.L. Smith, K. Natesan, Influence of nonmetallic impurity elements on the compatibility of liquid lithium with potential CTR containment materials. *Nuclear Technology*. 22, 392-404 (1974); <https://doi.org/10.13182/nt74-a31423>.
- [27] H.J. Goldshmidt, Interstitial alloys [transl. from English. S.N. Gorina]. Mir, Moscow, Vol. II. (1971) (in Russian).
- [28] P.J. Harward, I.M. George, Determination of $\beta/\beta+\gamma$ eutectoid transition temperature in ZrO_{2-x} at variable heating/cooling rates. *J. Nucl. Mater.* 265(1-2), 65-68 (1999); [https://doi.org/10.1016/s0022-3115\(98\)00620-5](https://doi.org/10.1016/s0022-3115(98)00620-5).
- [29] P.J. Harward, I.M. George, Dissolution of ZrO_2 in molten Zircaloy-4. *J. Nucl. Mater.* 265(1-2), 69-77 (1999); [https://doi.org/10.1016/s0022-3115\(98\)00512-1](https://doi.org/10.1016/s0022-3115(98)00512-1).
- [30] A. Wells, Structural Inorganic Chemistry. In 3 volumes. Vol. 2. Mir, Moscow (1987).
- [31] T. Arima, K. and et., Oxidation kinetics of Zircaloy-2 between 450°C and 600°C in oxidizing atmosphere. *J. Nucl. Mater.* 257(1), 67-77 (1998); [https://doi.org/10.1016/s0022-3115\(98\)00069-5](https://doi.org/10.1016/s0022-3115(98)00069-5).
- [32] I.I. Kornilov, V.V. Glazova, E.M. Kenina, Effect of Oxygen on the Properties of Zirconium at Elevated Temperatures. *Atomic Energy* 26(4), 324-327 (1969).
- [33] G.M. Hood, Point defect diffusion in α -Zr. *J. Nucl. Mater.* 159, 149-175 (1988); [https://doi.org/10.1016/0022-3115\(88\)90091-8](https://doi.org/10.1016/0022-3115(88)90091-8).
- [34] A. Shmakov, B. Kalin, E. Smirnov, Hydrogen in Zirconia Alloys. Hydride Embrittlement and Fracture of Zirconia (Russian Edition). Lambert Academic Publishing, Chisinau (2014). ISBN 978-3659532665.
- [35] M.V. Koteneva, Structure and destruction of oxide films of zirconium alloys: abstract of dissertation for the competition. Doctoral Thesis. National Research Technological University MISiS, Moscow, (2014).
- [36] J. Zhang, A.R. Oganov, X. Li, H. Dong, Q. Zeng, Novel compounds in the Zr-O system, their crystal structures and mechanical properties. *Physical Chemistry Chemical Physics* 17(26), 17301-17310 (2015); <https://doi.org/10.1039/c5cp02252e>.
- [37] B. Puchala, A. Van der Ven, Thermodynamics of the Zr-O system from first-principles calculations. *Physical Review B* 88(9), 094108 (2013); <https://doi.org/10.1103/physrevb.88.094108>.

- [38]D. Lee, P.T. Hill, Effect of oxygen on the fatigue behavior of Zircaloy. *J. Nucl. Mater.* 60(2), 227-230 (1976); [https://doi.org/10.1016/0022-3115\(76\)90170-7](https://doi.org/10.1016/0022-3115(76)90170-7).
- [39]R. Chosson, A.F. Gourgues-Lorenzon, V. Vandenberghe, J.C. Brachet, J. Crépin, Creep flow and fracture behavior of the oxygen-enriched alpha phase in zirconium alloys. *Scripta Materialia* 117, 20-23 (2016); <https://doi.org/10.1016/j.scriptamat.2016.02>.
- [40]S.A. Nikulin, A.B. Rozhnov, A.Y. Gusev, T.A. Nechaykina, S.O. Rogachev, M.Y. Zadorozhnyy, Fracture resistance of Zr-Nb alloys under low-cycle fatigue tests. *J. Nucl. Mater.* 446(1-3), 10-14 (2014); <https://doi.org/10.1016/j.jnucmat.2013.11.039>.
- [41]V.S. Vakhrusheva, O.A. Kolenkova, G.D. Sukhomlin, Influence of oxygen content on ductility, damageability and parameters of acoustic emission of metal pipes from Zr-1%Nb alloy. *Problems of atomic science and technology* 5, 104-109 (2005); https://vant.kipt.kharkov.ua/ARTICLE/VANT_2005_5/article_2005_5_104.pdf.
- [42]M. Liyanage, R. Miller, R.K.N.D. Rajapakse, Effect of Oxygen on Hydrogen Diffusivity in α -Zirconium. *arXiv:1909.02486v1 [cond-mat.mtrl-sci]* (2019); <https://arxiv.org/pdf/1909.02486.pdf>.
- [43]J. Desquines. V. Georgenthum. F. Lemoine. B. Cazalis, The fracture and spallation of zirconia layers in high burnup PWR fuel claddings submitted to RIA transients. Proceedings of 18th International Conference on Structural Mechanics in Reactor Technology (SMiRT 18) (Beijing, China, August 7-12, 2005); https://www.academia.edu/18675979/the_fracture_and_spallation_of_zirconia_layers_in_high_burnup_pwr_fuel_claddings_submitted_to_ria_transients.
- [44]P. Rudling, Zr alloy corrosion hydrogen pickup. ANT International, Molnlycke, Sweden, p. 96 (2013); <https://www.nrc.gov/docs/ML1525/ML15253A227.pdf>.
- [45]I. Aitchison, P.H. Davies, Role of microsegregation in fracture of cold-worked Zr-2,5% Nb pressure tubes II. *J. Nucl. Mater.* 203(3), 206-220 (1993); [https://doi.org/10.1016/0022-3115\(93\)90377-b](https://doi.org/10.1016/0022-3115(93)90377-b).
- [46]A.V. Nikulina, M.M. Perehud, B.K. Shamardin, V.P. Kobylansky, Metallurgical factors that determine the properties of zirconium alloys under irradiation. Proceedings of II International Conference on Reactor Materials Science (Alushta, May 22-25, 1990), Kharkov Physical-Technical Institute (KIPT), Kharkov, Vol. 4, p. 40-54 (1990) (in Russian); https://inis.iaea.org/collection/NCLCollectionStore/_Public/24/052/24052907.pdf.
- [47]V.P. Kobylansky, V.K. Shamardin, Z.E. Ostrovsky, V.M. Raevsky, A.B. Nikulina, M.M.Perehud, V.M. Grigoriev, Radiation forming of cladding and channel pipes from zirconium alloys at high neutron fluences. Proceedings of II International Conference on Reactor Materials Science, (Alushta, May 22-25, 1990), Kharkov Physical-Technical Institute (KIPT), Kharkov, Vol. 4, p. 64-72 (1990) (in Russian).
- [48]V.A. Tsikalov, B.V. Samsonov, A.Ya. Rogozyanov, P.P. Losev, V.C. Shamardin, V.P.Kobylansky, A.V. Nikulina, M.B. Thebesian, Influence of Reactor Irradiation on Mechanical Properties of Zirconium Alloys. *Physics and chemistry of material processing* 6, 3-7 (1982) (in Russian).
- [49]E.M. Tararaeva, L.S. Muravieva, Influence of oxygen and tin on the mechanical properties of zirconium alloys with 1 and 2.5% Nb. In book: Structure and properties of alloys for nuclear power engineering / Ed. O.S. Ivanova, T.A. Babaev. Nauka, Moscow, (1973) (in Russian).
- [50]R.F. Voitovich, Oxidation of zirconium and its alloys. Naukova Dumka, Kyiv, (1989) (in Russian).
- [51]O. Blahova, R. Medlin, J. Riha, Evaluation of microstructure and local mechanical properties of zirconium alloys. In: 18th International Conference on Metallurgy and Materials (May 19th - 21st 2009). Proceedings. Metal-2009. Červený Zámek, Hradec nad Moravicí, Czech Republic, 19–21.5.2009 (2009); http://metal2013.tanger.cz/files/proceedings/metal_09/Lists/Papers/084_e.pdf.
- [52]M. Steinbrück, M. Große, Deviations from parabolic kinetics during oxidation of zirconium alloys. Zirconium in the Nuclear industry : Proceedings of 17th International Symposium on Zirconium in the Nuclear Industry, ASTM International, West Conshohocken, p. 979 (2014); <https://doi.org/10.1520/STP154320130022>.
- [53]M. Steinbrueck, F.O. da Silva, M. Grosse, Oxidation of Zircaloy-4 in steam-nitrogen mixtures at 600–1200 °C. *J. Nucl. Mater.* (2017); <https://doi.org/10.1016/j.jnucmat.2017.04.034>.
- [54]O.M. Ivasishin, V.N. Voyevodin, A.I. Dekhtyar, P.E. Markovsky, M.M. Pylypenko, S.D.Lavrinenko, R.G. Gontareva, Peculiarities of Mechanical Behavior of Fuel Rod Tubes Made of Zr-1%Nb Alloy under Conditions of Emergency Shutdown Simulation of Cooling. *Problems of atomic science and technology* 5(99), 53 (2015); <http://dspace.nbu.gov.ua/bitstream/handle/123456789/112292/10-Ivasishin.pdf>.
- [55]M. Steinbrück, High-temperature reaction of oxygen-stabilized α -Zr(O) with nitrogen. *J. Nucl. Mater.* 447(1-3), 46-55 (2014); <https://doi.org/10.1016/j.jnucmat.2013.12.024>.
- [56]J. Benard, L'oxydation des Metaux, Tom. II, Gauthiers Villard, Paris, (1964).
- [57]J. Birchley, L. Fernandez-Moguel, Simulation of air oxidation during a reactor accident sequence: Part 1 – Phenomenology and model development. *Annals of Nuclear Energy* 40(1), 163-170 (2012); <https://doi.org/10.1016/j.anucene.2011.10.019>.
- [58]S. Yu, Q. Zeng, A. R. Oganov, G. Frapper, B. Huang, H. Niu, L. Zhang, First-principles study of Zr–N crystalline phases: phase stability, electronic and mechanical properties. *RSC Advances* 7(8), 4697-4703 (2017); <https://doi.org/10.1039/c6ra27233a>.
- [59]A. A. Gromov, Patterns of the processes of obtaining nitrides and oxynitrides of elements of III and IV groups: a study guide, Publishing House of Tomsk Polytechnic University, Tomsk, (2009) (in Russian); https://portal.tpu.ru/departments/otdel/publish/izdaniya_razrabotanye_v_ramkah_IOP/Tab/zakonom_proz_zachita.pdf.

- [60] Van Lam Do, Thi Mai Dung Do & Toru Ogawa, Features of Zr-rich corner of the Zr-N-O ternary system by controlled low-pressure oxidation and thermodynamic analysis. *Journal of Nuclear Science and Technology* 1-11 (2017); <https://doi.org/10.1080/00223131.2017.1315974>.
- [61] Yu.G. Zanulin, Areas of homogeneity of zirconium oxide nitride with NaCl structure type at 1500°C. *Zh. Neorg. Khim.* 16, 315-317 (1971). (in Russian).
- [62] A. Ermoline. Experimental technique for studying high-temperature phase equilibria in reactive molten metal based systems. Dissertation 669. New Jersey Institute of Technology, Newark, New Jersey, USA, (2005); <https://digitalcommons.njit.edu/cgi/viewcontent.cgi?article=1724&context=dissertations>.
- [63] V.S. Trush, V.N. Fedirko, A.G. Luk'yanenko, M.A. Tikhonovsky, P.I. Stoev. Influence of thermochemical treatment on properties of tubes from Zr-1Nb alloy. *Problems of atomic science and technology* 114(2), 70-75 (2018).
- [64] V.S. Trush, O.H. Lukianenko, P.I. Stoev, Influence of modification of the surface layer by penetrating impurities on the long-term strength of Zr-1% Nb Alloy, *Materials Science* 55(4), 585-589 (2020); <https://doi.org/10.1007/s11003-020-00342-z>.
- [65] V.M. Fedirko, O.H. Luk'yanenko, V.S. Trush, Influence of the diffusion saturation with oxygen on the durability and long-term static strength of titanium alloys, *Materials science* 50(3), 415-420 (2014); <https://doi.org/10.1007/s11003-014-9735-2>.
- [66] V.N. Fedirko, A.G. Luk'yanenko, V.S. Trush, Solid-solution hardening of the surface layer of titanium alloys. Part 1. Effect on mechanical properties, *Metal Science and Heat Treatment* 56(7), 368-373 (2014); <https://doi.org/10.1007/s11041-014-9764-3>.
- [67] I.M. Pohrelyuk, J. Padgurskas, O.V. Tkachuk, A.G. Luk'yanenko, V.S. Trush, S.M. Lavryś, Influence of oxynitriding on antifriction properties of Ti-6Al-4V titanium alloy, *Journal of friction and wear* 4(41), 333-337 (2020); <https://doi.org/10.3103/s1068366620040108>.

В.С. Труш¹, М.М. Пилипенко², П.І. Стоєв², М.А. Тихоновський², І.М. Погрелюк¹,
В.М. Федірко¹, О.Г. Лук'яненко¹, С.М. Лаврись¹

Вплив елементів проникнення (кисню, азоту) на властивості цирконієвих сплавів (літературний огляд)

¹Фізико-механічний інститут ім. Г.В. Карпенка НАН України, Львів

²Інститут фізики твердого тіла, матеріалознавства та технологій ННЦ «ХФТІ» НАН України, Харків,
trushvasyl@gmail.com

Наведено літературний огляд закономірностей впливу елементів проникнення (кисню, азоту) на властивості цирконієвих сплавів. Наголошено, що у науково-технічній літературі основну увагу приділено об'ємному легуванню цирконієвих сплавів киснем та азотом. Показано, що цирконій з азотом та киснем утворює ряд стабільних сполук субоксидів та субнітридів. Наведено фізико-механічні характеристики цирконію після обробки в середовищах, що містять одночасно кисневу та азотну компоненти.

Ключові слова: цирконієві сплави, кисень, азот, розчинність, фізико-механічні властивості.